

pubs.acs.org/acsagscitech Letter

# Inactivated Plant Viruses as an Agrochemical Delivery Platform

Paul L. Chariou, Yifeng Ma, Michael Hensley, Erin N. Rosskopf, Jason C. Hong, Raghavan Charudattan, and Nicole F. Steinmetz\*

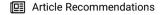


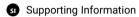
**Cite This:** ACS Agric. Sci. Technol. 2021, 1, 124–130



**ACCESS** 

Metrics & More





ABSTRACT: Nanoparticle-based pesticide delivery systems have emerged to decrease the environmental and health impact of pesticides while increasing their efficacy. A majority of nanopesticides in the development pipeline are synthetic materials, some of which present their own environmental risks. We propose the development of naturally occurring nanomaterials, namely plant viruses such as tobacco mild green mosaic virus (TMGMV), for the delivery of pesticides. We and others have previously shown that plant virus-based nanoparticles have favorable soil mobility properties and thus could offer new avenues for the delivery of pesticides to target root-feeding pests. Toward the application of plant virus-based vectors as pesticide delivery agents, we optimized inactivation methods. We report the successful inactivation of TMGMV using 10 J cm<sup>-2</sup> of ultraviolet light, 1.5 M  $\beta$ PL, or 1 M formalin; the lack of infectivity was confirmed using *Nicotiana tabacum* Tennessee 86, *N. tabacum* Samsun nn, and tropical soda apple (*Solanum viarum*).

KEYWORDS: tobacco mild green mosaic virus, viral inactivation, UV light,  $\beta$ -propiolactone, formalin, precision farming, nanocarrier, pesticide delivery

#### INTRODUCTION

Biological pests, including microbes, arthropods, nematodes, and weeds, are responsible for major losses in crop yields. In modern agriculture, pest management often relies on the use of synthetic chemicals that are sparingly soluble and adsorb to soil particles with high affinity. Contemporary pesticides generally have poor bioavailability and require applications in large quantities to achieve an effective dose. The accumulation of these chemicals in the environment contaminates both land and water resources, which leads to off-target toxicity to other species, including domestic animals and humans (e.g., cancer and infertility). As a result, an increasing number of pesticides have been withdrawn from the market. Because these compounds are not being efficiently replaced, there is currently a gap in the market that threatens our food safety and security.

Advances in nanotechnology have led to the development of agrochemical nanomaterials to protect crops from various pests. The encapsulation or conjugation of pesticides in(to) nanocarriers improves their stability and solubility, preventing their premature degradation by photolysis or biodegradation. While nanocarriers can provide significant benefits to the agricultural industry, some health and environmental risks remain to be mitigated. A majority of nanopesticides in the development pipeline are based on metallic compounds, synthetic or natural polymers, which tend to persist in the environment and in some cases can cause acidification of soil, impairing its fertility.<sup>6,7</sup> We and others have proposed to repurpose the capsids of plant viruses for pesticide delivery applications. For example, the delivery of anthelmintic drugs to endoparasitic nematodes using the icosahedral red clover necrotic mosaic virus (RCNMV)<sup>8</sup> and the rod-shaped tobacco mild green mosaic virus (TMGMV)<sup>9</sup> has been reported. We also demonstrated that TMGMV exhibits good soil mobility leading

to accumulation at the crop root level, where pests such as nematodes reside. Plant viruses are already part of the natural soil ecosystem and are not known to cause adverse effects in humans or animals.

While infectious TMGMV has been approved by the U.S. Environmental Protection Agency for use as a bioherbicide against tropical soda apple (TSA) weed, 11,12 for pesticide delivery a non-infectious formulation would be most desired to enable broad applicability. Therefore, in this work we report the formulation of inactivated TMGMV. Previous reports on the inactivation of plant viruses have focused on chemical treatments such as formalin, hydrogen peroxide, or even sodium nitrite. 13 Generally, these chemical treatments either cross-link or oxidize the nucleic acids and/or proteins. In addition, ultraviolet (UV) radiation is a powerful tool for the inactivation of plant viruses and has been demonstrated to inactivate tobamoviruses. 14-22 UV irradiation causes RNA-protein crosslinks as well as dimerization of adjacent uracils, both of which inhibit RNA replication and translation.<sup>23</sup> While UV inactivation studies have been performed using TMGMV, data relied on visual local lesion quantification to record the level of infectivity after viral inactivation; this method has now been outperformed by far more sensitive assays such as reverse-transcription polymerase chain reaction (RT-PCR), which detects the presence of viral RNA within the inoculated leaves. Therefore,

Received: April 12, 2021 Revised: May 19, 2021 Accepted: May 20, 2021 Published: May 28, 2021





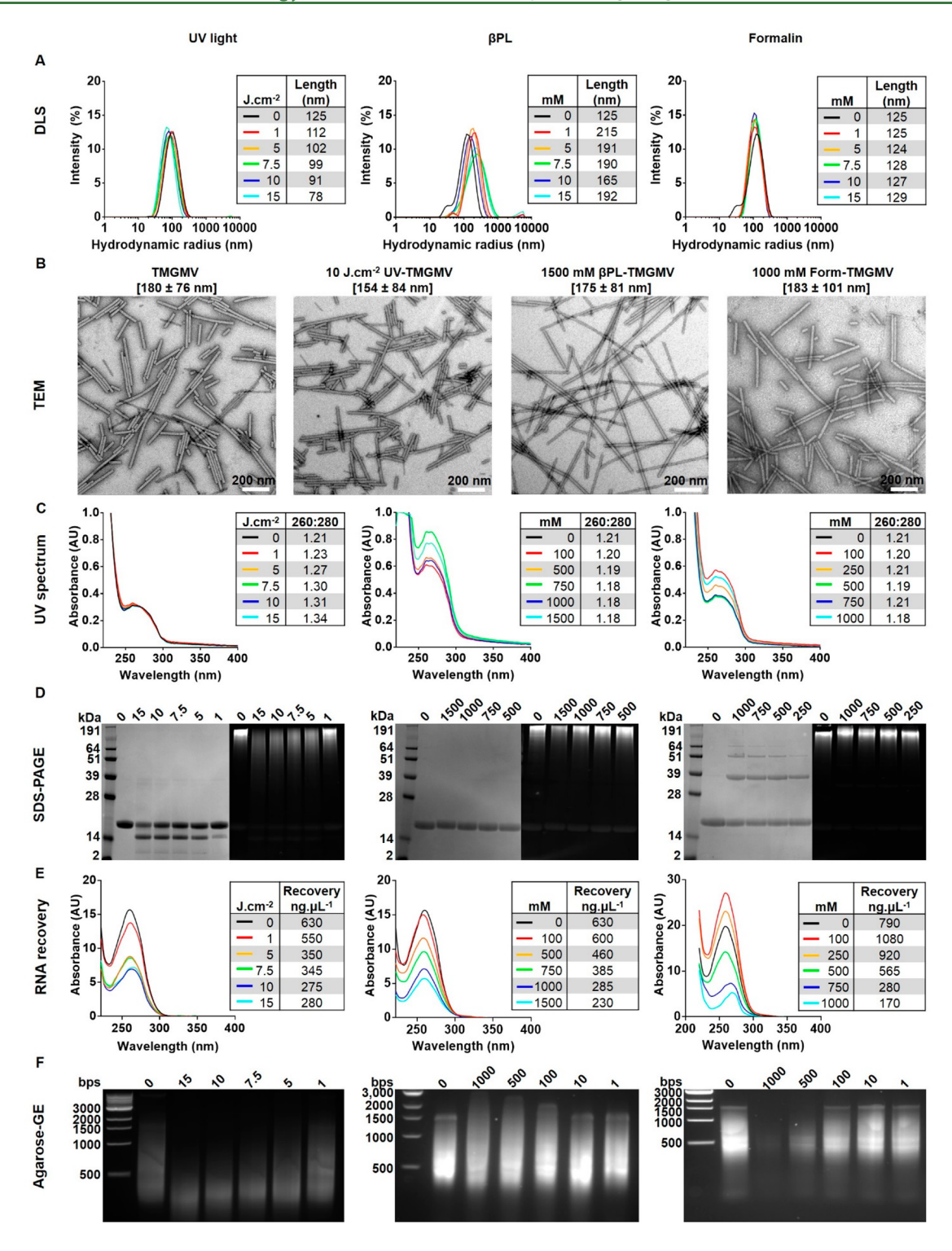


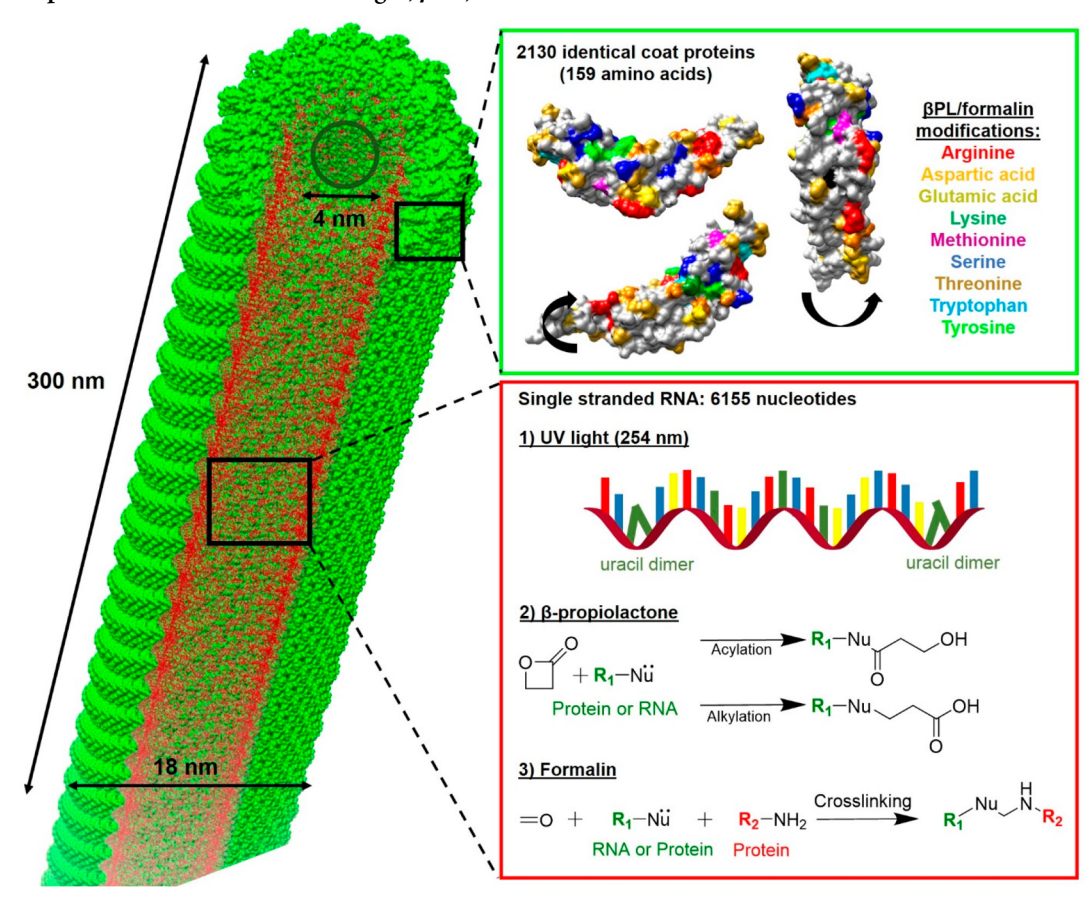
Figure 1. Characterization of inactivated TMGMV. (A) Dynamic light scattering of TMGMV treated with (left) UV light (0, 1, 5, 7.5, 10, and 15 J cm<sup>-2</sup>), (middle) βPL (0, 100, 500, 750, 1000, and 1500 mM), and (right) formalin (0, 100, 250, 500, 750, and 1000 mM). (B) TEM images of the inactivated TMGMV formulations (negatively stained). Scale bars correspond to 200 nm. (C) UV–visible light spectra of native and inactivated TMGMV. (D) Denaturing sodium dodecyl sulfate–polyacrylamide gel electrophoresis gels under white light after Coomassie staining (protein detection) and under UV light after GelRed staining (RNA detection). (E) UV–visible light spectra of RNA extracted from native and inactivated TMGMV. (F) Agarose-GE gels of the RNA extracted from UV-TMGMV, βPL-TMGMV, and formalin-TMGMV, under UV light after GelRed staining (RNA detection).

follow-up studies to define the effective dose range were warranted.

Here, we performed dose-escalation studies to determine the effective dose required to inactivate TMGMV particles by UV

light versus chemical treatment using  $\beta$ -propiolactone ( $\beta$ PL) or formalin; the chemical inactivation methods have not yet been applied to TMGMV. We determined the minimal effective dose and also considered the structural stability and chemical

Scheme 1. Comparison of the Effects of UV Light,  $\beta$ PL, and Formalin on TMGMV<sup>a</sup>



<sup>a</sup>Left, structure of TMGMV using UCSF Chimera (Protein Data Bank entry 1VTM) depicting the coat proteins in green and the RNA in red. At the top right is a single coat protein in three different orientations, highlighting amino acids that could be potentially modified by  $\beta$ PL and/or formalin. At the bottom right, (1) inactivation of RNA using 254 nm UV light to promote uracil dimers. In the RNA schematic, adenine is colored blue, uracil green, cytosine yellow, and guanine red. (2)  $\beta$ PL-induced acylation and alkylation of RNA and proteins. (3) Formalin-induced cross-linking of RNA and proteins.

properties of the inactive TMGMV. Longitudinal stability studies were also carried out to confirm that the inactivated TMGMV remained non-infectious after extended storage.

# RESULTS AND DISCUSSION

Dose-escalation studies using UV light,  $\beta$ PL, and formalin were performed, and the resulting inactivated TMGMV particles were characterized by dynamic light scattering (DLS), transmission electron microscopy (TEM), and size exclusion chromatography (SEC) to assess their physical state (Figure 1A,B, Figures S1-S3, and Scheme 1). Independent of the treatment modality or concentration, SEC indicated intact TMGMV particles; free coat proteins or broken particles were not detected (it should be noted that the resolution of the Superose 6 column does not allow the measurement of potential particle aggregation). The elution profile was consistent with native TMGMV and native or treated TMGMV particles eluted at ~8 mL from the Superose 6 column (Figures S1-S3). As a complementary method, DLS was used to determine the hydrodynamic radius of TMGMV; DLS provides insight into the TMGMV formulation and its possible aggregation state, albeit an estimated measure given the high-aspect ratio shape of TMGMV. DLS revealed signs of particle breakage when UV-TMGMV was treated with large doses of UV light (Figure 1A). There was a trend that the average hydrodynamic radius of TMGMV decreased from 125

nm to 112, 102, 99, 91, and 78 nm with increasing UV doses of 0, 1, 5, 7.5, 10, and 15 J cm<sup>-2</sup>, respectively. DLS also revealed signs of particle aggregation in the  $\beta$ PL-TMGMV formulations (Figure 1A); compared to native TMGMV (125 nm average),  $\beta$ PL-TMGMV exhibited hydrodynamic radii between 165 and 215 nm in samples treated with 0, 100, 500, 750, 1000, and 1500 mM  $\beta$ PL. In contrast, formalin-treated TMGMV (Form-TMGMV) showed no signs of particle breakage or aggregation with average lengths of 125–129 nm in samples treated with 0, 100, 250, 500, 750, and 1000 mM formalin (Figure 1A).

The polydispersity of TMGMV as observed by TEM was consistent with our previous observations  $^{10}$  and was attributed to the methods used to produce and purify TMGMV, as well as the process by which the particles were dried during the preparation of the TEM grids (Figure 1B). TEM data concurred with the observations made by DLS. While the native TMGMV averaged a size of 180  $\pm$  76 nm, the UV-TMGMV (154  $\pm$  84 nm) revealed signs of breakage, and Form-TMGMV (183  $\pm$  101 nm) retained its structural integrity.  $\beta$ PL-TMGMV (175  $\pm$  81 nm) did not show signs of aggregation but rather formed a head-to-tail self-assembling filament. This phenomenon was previously reported using TMV assisted by aniline polymerization and was attributed to a combination of hydrophobic interactions, electrostatic forces between the dipolar ends of adjacent particles.  $^{24}$  We hypothesize that the acylation and

alkylation of amino acid residues (Figure S4) toward the opposite ends of TMGMV promote such interactions.

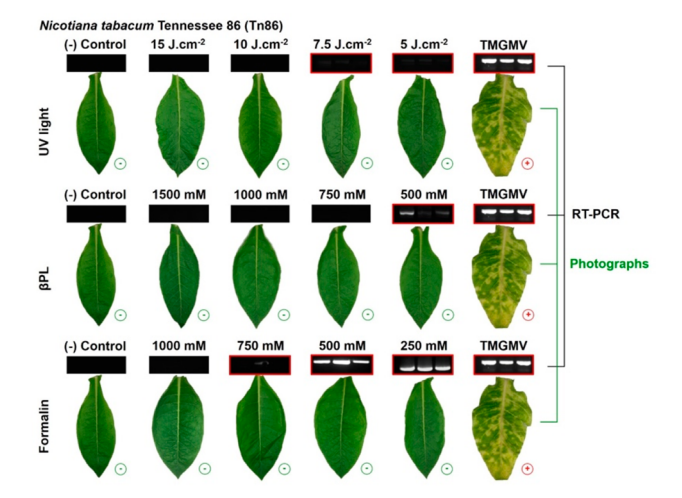
Next, we assessed the RNA state after UV,  $\beta$ PL, and formalin treatment. TMGMV contains a positive-sense, single-stranded RNA genome of 6355 nucleotides and contains more than 400 sites of adjacent uracils prone to dimerization (Figure S5). Overall, UV-visible spectroscopy indicated that the RNA:protein ratio (260 nm:280 nm absorbance ratio) of  $\beta$ PL-TMGMV and Form-TMGMV remained close to 1.2, indicating no degradation or loss of RNA, as expected (Figure 1C). UV-TMGMV suffered from an increase in the 260 nm:280 nm ratio from 1.2 to 1.3. This change was attributed to coat protein breakage, as was observed in the gel electrophoresis experiments (Figure 1D). Sodium dodecyl sulfate-polyacrylamide gel electrophoresis gels were imaged following staining for nucleic acid and proteins under UV light and white light, respectively. While the coat proteins of TMGMV are ~17 kDa in size, a second protein band (~14 kDa) was observed in the UV-TMGMV-treated samples, and its intensity increased with UV dosage. It should be noted that free coat protein could not be detected by SEC (Figure S1); therefore, the smaller coat protein may be partially broken yet still assembled in the nucleoprotein complex. Identification of the amino acid sequence of the ~14 and ~17 kDa bands by matrix-assisted laser desorption/ ionization time-of-flight mass spectrometry (MALDI-TOF/ MS) was inconclusive as it was not able to clearly resolve the bands, and thus, we could not obtain pure samples for analysis.

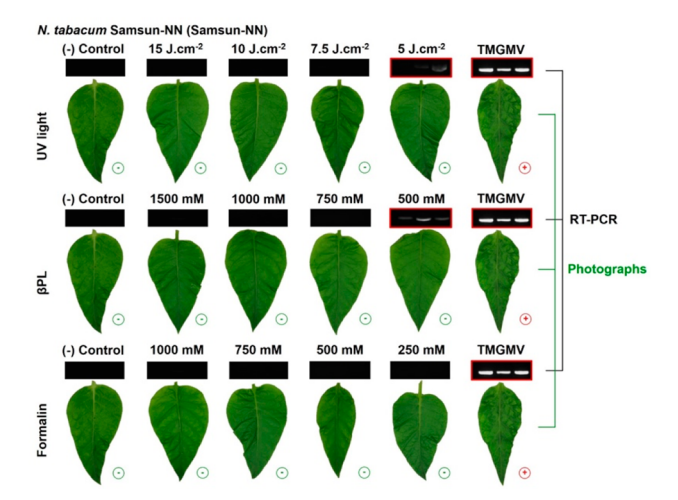
Denatured  $\beta$ PL-TMGMV coat proteins showed no sign of protein breakage or aggregation regardless of the  $\beta$ PL dose used. In contrast, the larger the dose of formalin, the more intercoat protein cross-linking was observed, as indicated by the presence of additional high-molecular weight bands. GelRed staining of the RNA content of TMGMV particles revealed no significant changes in RNA motility in  $\beta$ PL-TMGMV and Form-TMGMV samples, but there were signs of RNA breakage in samples treated with UV doses above 1 J cm<sup>-2</sup> (Figure 1D). The genome content of each formulation was further analyzed following RNA extraction from the TMGMV formulations on native agarose gels (Figure 1E,F). Treatment doses of >1 J cm<sup>-2</sup> of UV or 10 mM  $\beta$ PL and 100 mM formalin led to significant RNA damage and a decrease in total RNA recovery.

On the basis of these biochemical data, we hypothesized that a minimum of 5 J cm<sup>-2</sup> of UV light, 100 mM  $\beta$ PL, and 500 mM formalin would have been required to inactivate TMGMV; at these concentrations, the overall structural integrity of the particles was maintained, but RNA damage was confirmed.

To confirm the dose of UV,  $\beta$ PL, or formalin required to inactivate TMGMV, three plant species susceptible to TMGMV infection were inoculated (Figure 2).

- (1) In *Nicotiana tabacum* Tennessee 86 (Tn86), which is a diagnostic species, TMGMV elicits a strong, bright, yellow and green foliar mosaic with occasional necrotic patches; the symptoms are obvious by visual inspection and allow for photographic documentation.
- (2) N. tabacum Samsun nn (Samsun nn) is also a diagnostic species as well as propagation species; it is the propagation host used by BioProdex to manufacture SolviNix (the TMGMV-based bioherbicide). While Samsun nn produces high yields of TMGMV (1–3 mg/g of fresh leaf tissue), the mosaic symptom in this host is mild and not always detectable by eye; it is quite difficult to photograph.
- (3) In tropical soda apple (TSA) (Solanum viarum), TMGMV elicits systemic necrosis that is almost invariable.





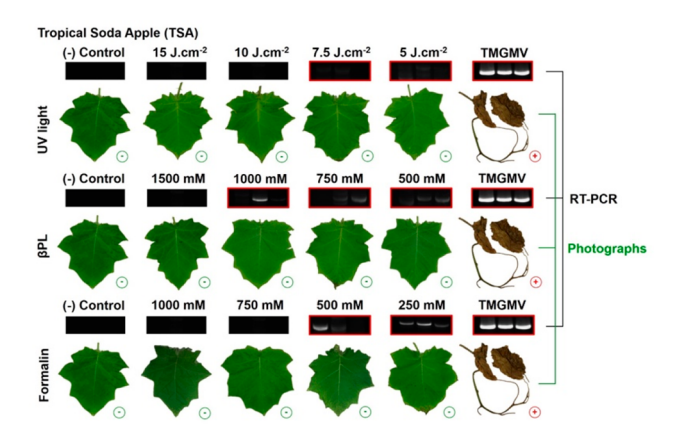


**Figure 2.** Analysis of the infectivity of TMGMV v. inactivated TMGMV against *N. tabacum* Tennessee 86 (Tn86), *N. tabacum* Samsun nn (Samsun nn), and tropical soda apple (TSA). Depiction of individual leaves infected with TMGMV, UV-TMGMV, βPL-TMGMV, or Form-TMGMV at various doses. A minus sign indicates leaves that were visually symptomless, while a plus sign represents infected leaves. RNA was extracted from leaves, and RT-PCR amplicons were obtained proportionally to the TMGMV infectivity level. RT-PCR results highlighted by red boxes depict conditions that were positive for TMGMV RNA within at least one leaf per condition.

Tn86, Samsun nn, and TSA were challenged with native or UV-treated or chemically treated TMGMV. Leaves were imaged

Table 1. Leaf Infectivity as Determined by Visual Inspection<sup>a</sup>

|            |             |                       | N. tabacı             | um Tennessee 86 (      | Tn86)                |                      |                                       |       |
|------------|-------------|-----------------------|-----------------------|------------------------|----------------------|----------------------|---------------------------------------|-------|
| UV light   | (-) control | 15 J cm <sup>-2</sup> | 10 J cm <sup>-2</sup> | 7.5 J cm <sup>-2</sup> | 5 J cm <sup>-2</sup> | 1 J cm <sup>-2</sup> | $0.2 \ \mathrm{J} \ \mathrm{cm}^{-2}$ | TMGMV |
|            | _           | _                     | _                     | _                      | _                    | +                    | _                                     | ++++  |
| $\beta$ PL | (-) control | 1500 mM               | 1000 mM               | 750 mM                 | 500 mM               | 100 mM               | 1 mM                                  | TMGMV |
|            | _           | _                     | _                     | _                      | _                    | +                    | ++                                    | ++++  |
| formalin   | (-) control | 1000 mM               | 750 mM                | 500 mM                 | 250 mM               | 100 mM               | 1 mM                                  | TMGMV |
|            | _           | _                     | _                     | _                      | _                    | _                    | ++                                    | ++++  |
|            |             |                       | N. tabacur            | n Samsun nn (Sam       | sun nn)              |                      |                                       |       |
| UV light   | (-) control | 15 J cm <sup>-2</sup> | 10 J cm <sup>-2</sup> | 7.5 J cm <sup>-2</sup> | 5 J cm <sup>-2</sup> | 1 J cm <sup>-2</sup> | $0.2 \ \mathrm{J} \ \mathrm{cm}^{-2}$ | TMGMV |
|            | _           | _                     | _                     | _                      | _                    | _                    | _                                     | ++++  |
| $\beta$ PL | (-) control | 1500 mM               | 1000 mM               | 750 mM                 | 500 mM               | 100 mM               | 1 mM                                  | TMGMV |
|            | _           | _                     | _                     | _                      | _                    | ++                   | +++                                   | ++++  |
| formalin   | (-) control | 1000                  | 750                   | 500                    | 250                  | 100                  | 1                                     | TMGMV |
|            | _           | _                     | _                     | _                      | _                    | +                    | ++                                    | ++++  |
|            |             |                       | tropi                 | cal soda apple (TS     | A)                   |                      |                                       |       |
| UV light   | (-) control | 15 J cm <sup>-2</sup> | 10 J cm <sup>-2</sup> | 7.5 J cm <sup>-2</sup> | 5 J cm <sup>-2</sup> | 1 J cm <sup>-2</sup> | $0.2 \ \mathrm{J} \ \mathrm{cm}^{-2}$ | TMGMV |
|            | _           | _                     | _                     | _                      | _                    | _                    | _                                     | ++++  |
| $\beta$ PL | (-) control | 1500 mM               | 1000 mM               | 750 mM                 | 500 mM               | 100 mM               | 1 mM                                  | TMGMV |
|            | _           | _                     | _                     | _                      | _                    | +++                  | +++                                   | ++++  |
| formalin   | (-) control | 1000 mM               | 750 mM                | 500 mM                 | 250 mM               | 100 mM               | 1 mM                                  | TMGMV |
|            | _           | _                     | _                     | _                      | _                    | _                    | +                                     | ++++  |

<sup>&</sup>lt;sup>a</sup>A minus sign indicates no symptoms, while plus signs indicate symptom levels.

and harvested individually ~20 days post-inoculation (Figure 2 and Table 1). Leaves inoculated with larger doses of UV-treated or chemically treated TMGMV showed no visual signs of infection in all three species. In addition to visual inspection for symptoms, RT-PCR was carried out on the total RNA content extracted from individual leaves to further attest to the presence of TMGMV infection or lack thereof (Figures S6-S8). A total of three leaves per treatment condition were selected randomly and analyzed by RT-PCR. This method is a more sensitive assay as opposed to visual inspection of the leaves; for example, visual inspection of the leaves may indicate a lack of apparent infection when using 5 J cm<sup>-2</sup> of UV, 500 mM  $\beta$ PL, or 500 mM formalin in either plant species tested. However, at these concentrations, the leaves were TMGMV positive using Tn86 and TSA plants. RT-PCR testing and analysis of the amplified DNA fragments by agarose gel electrophoresis confirmed the inactivating UV dose for TMGMV to be  $7.5-10 \,\mathrm{J}\,\mathrm{cm}^{-2}$ , and this was consistent for the three plant species tested. Differences were noted for the chemically inactivated TMGMV preparations. While 750 mM  $\beta$ PL was enough to inactivate TMGMV and prevents infection of Tn86 and Samsun nn, 1500 mM  $\beta$ PL was required to prevent TMGMV infection in the hypersensitive TSA. Therefore, one could inactivate TMGMV using 750 mM  $\beta$ PL and still use it as a bioherbicide with high specificity against TSA, which may be an interesting extension of the current formulation. Formalin was the least consistent treatment modality and required doses varying of 1000, 250, and 750 mM to inactivate Tn86, Samsun nn, and TSA, respectively. Overall, the required treatment doses to prevent infection in all three plant species were 10 J cm<sup>-2</sup> of UV, 1.5 M  $\beta$ PL, and 1 M formalin. However, given the variability of formalin dosage needed to achieve inactivation, this may be the least favorable to use for commercialization.

Next, we determined whether inactivated TMGMV remained inactivated and structurally intact during storage. A longitudinal study was carried out, in which native TMGMV and inactivated TMGMV were stored in KP buffer at 4 °C and samples were removed and characterized at the following time points: 1 day, 1 week, 3 months, 4 months, 5 months, and 6 months post-

treatment using SEC, DLS, and TEM methods, as described above (Figures S9–S14). The overall data indicate that TMGMV remained intact during storage; aggregation or disassembly was not observed. However, it was noted that the average length of UV-,  $\beta$ PL-, and formalin-inactivated TMGMV decreased over the 6-month time frame; 32%, 34%, and 14% decreases in length were observed for UV-,  $\beta$ PL-, and Form-TMGMV, respectively (for a detailed discussion, see the Supporting Information). The infectivity of the freshly inactivated TMGMV was compared to their 6-month old counterparts, and plant challenge studies indicate that the inactivated TMGMV preparations are suitable for storage (Figure 15 and Table S2). However, one has to consider the shortening of the nanoparticles that may impact soil and plant distribution and pesticide loading.

All three treatment modalities have advantages and disadvantages in terms of manufacturing (Table S3). UV treatment is the cheapest, fastest, and most reproducible inactivation modality but leads to shortening of the particles; 10 J cm<sup>-2</sup> UV-TMGMV particles are on average 30 nm shorter than native TMGMV (or in other words 10% shorter than the native TMGMV). In contrast,  $\beta$ PL treatment maintains particle integrity, although it leads to end-to-end alignment of TMGMV. Furthermore,  $\beta PL$  is an expensive and biohazardous chemical; the chemical treatment also requires additional purification steps, therefore reducing yields by 40-60%. Similarly, formalin maintains particle integrity but requires a long treatment incubation (5 days); the additional purification steps required to remove the treatment reagents are also at the cost of lower yields (40–60%). Formalin treatment gave the least consistent inactivation results among different plant species and therefore may require careful optimization for each species of interest. Altogether, UV inactivation may be the most suitable; it could be easily integrated into the purification process.

The inactivation of TMGMV by UV light has been reported in the 20th century using the focal lesion quantification method. These studies reported using different sources of UV light with various intensities and power settings, which

makes it difficult to compare the results. In addition, the time of UV exposure was recorded to assess UV inactivation instead of the more accurate joules per square centimeter units of measure; for example, Ginoza et al. reported full inactivation of TMGMV after UV exposure for 2 min, while Streeter et al. stated that a 6 min exposure was required. Using our system, UV exposure for 2 and 6 min would correspond to  $\sim$ 1 and  $\sim$ 2.5 J cm $^{-2}$ , respectively. At these concentrations, the leaves appear symptomless but RT-PCR revealed the presence of infectious TMGMV (Figures S6–S8).

The plant virus cowpea mosaic virus (CPMV) has been shown to be inactivated at UV doses of 2.5-5 J cm<sup>-2,23,25</sup> CPMV consists of a bipartite ssRNA virus forming a 31 nm icosahedron with pseudo T = 3 symmetry. The differences in the UV dose required to yield inactivated virus preparations can be explained by differences in virus structure and assembly: CPMV's ssRNA genome is encapsulated into the internal cavity of the capsid; in contrast, TMGMV's genome is incorporated into the nucleoprotein assembly. Thus, the TMGMV is somewhat buried in the coat protein structure, which likely confers enhanced stability. The reported inactivation of mammalian viruses such as influenza (ssRNA, ~1 J cm<sup>-2</sup>),<sup>26</sup> HIV (ssRNA, ~1 J cm<sup>-2</sup>),<sup>27</sup> and hepatitis A (ssRNA, ~0.3 J cm<sup>-2</sup>)<sup>28</sup> required smaller doses, which may reflect the less robust structure of mammalian viruses that did not evolve to persist under changing environmental conditions.

βPL and formalin are more commonly used to produce nonvirulent mammalian virus vaccines. <sup>29,30</sup> Compared to plant viruses, many mammalian viruses have a lipid envelope that can be cross-linked by formalin or acylated/alkylated by βPL; thus, they generally require smaller treatment doses to be inactivated. For example, equine herpesvirus type  $I_s^{31}$  eastern equine encephalitis and poliomyelitis type  $I_s^{32}$  HIV, <sup>33</sup> and the influenza virus were successfully inactivated with 5–60 mM βPL. Hepatitis  $A_s^{35}$  Japanese encephalitis virus, <sup>36</sup> HIV, <sup>33</sup> influenza A virus, <sup>37</sup> and rabies were also successfully treated with 5–120 mM formalin. It is the structural integrity of TMGMV that makes it attractive for exploitation in nanoengineering and environmental applications; however, these same features make it harder, yet not impossible, to generate inactivated TMGMV preparations; the dose required was ~10-fold larger than those of the previously mentioned mammalian vaccines.

# CONCLUSIONS

To date, TMGMV is the only plant viral nanoparticle that has been approved by the U.S. Environmental Protection Agency for use as a bioherbicide. To advance and broaden the use of TMGMV as a potential pesticide nanocarrier, we addressed its potential nontarget risk by producing a set of inactivated TMGMV formulations. TMGMV was inactivated with 10 J cm<sup>-2</sup> of UV light, 1500 mM  $\beta$ PL, and 1000 mM formalin, laying the groundwork for the development of eco-friendly and non-infectious viral pesticide nanocarriers.

## ASSOCIATED CONTENT

#### Supporting Information

The Supporting Information is available free of charge at https://pubs.acs.org/doi/10.1021/acsagscitech.1c00083.

FPLC results (Figures S1–S3 and S9–S12), virus structure (Figure S4), genome sequence of TMGMV (Figure S5), agarose gels (Figures S6–S8), characterization of inactivated TMGMV after storage (Figures S9–

S14), infectivity of TMGMV after storage (Figure S15), Materials and Methods, RT-PCR protocol (Table S1), a summary of previous publications (Table S2), and comparison of methods used for inactivation (Table S3) (PDF)

# AUTHOR INFORMATION

## **Corresponding Author**

Nicole F. Steinmetz — Department of Bioengineering,
Department of NanoEngineering, Department of Radiology,
Moores Cancer Center, Center for Nano-ImmunoEngineering,
and Institute for Materials Discovery and Design, University of
California, San Diego, La Jolla, California 92039, United
States; ◎ orcid.org/0000-0002-0130-0481;
Email: nsteinmetz@ucsd.edu

#### **Authors**

Paul L. Chariou — Department of Bioengineering, University of California, San Diego, La Jolla, California 92039, United States

Yifeng Ma — Department of NanoEngineering, University of California, San Diego, La Jolla, California 92039, United States

Michael Hensley — U.S. Horticultural Research Laboratory, Agricultural Research Service, U.S. Department of Agriculture, Fort Pierce, Florida 34945, United States

Erin N. Rosskopf — U.S. Horticultural Research Laboratory, Agricultural Research Service, U.S. Department of Agriculture, Fort Pierce, Florida 34945, United States

Jason C. Hong – U.S. Horticultural Research Laboratory, Agricultural Research Service, U.S. Department of Agriculture, Fort Pierce, Florida 34945, United States

Raghavan Charudattan – BioProdex, Inc., Gainesville, Florida 32609, United States; Plant Pathology, University of Florida, Gainesville, Florida 32611, United States

Complete contact information is available at: https://pubs.acs.org/10.1021/acsagscitech.1c00083

## **Author Contributions**

N.F.S. devised and oversaw the project, the main conceptual ideas, and proof outline. P.L.C. and Y.M. developed the technical procedures and performed the experiments. M.H., E.N.R., J.C.H., and R.C. performed the plant growth, maintenance, inoculation, and harvest. P.L.C. and N.F.S. wrote the manuscript. All authors read or edited the manuscript.

# **Funding**

This work was supported in part by National Institute of Food and Agriculture (NIFA) Grant 2020-67021-31255 (to N.F.S.) and grants from the National Science Foundation: CAREER DMR-1841848 (to N.F.S.) and through the UC San Diego Materials Research Science and Engineering Center (UCSD MRSEC) (DMR-2011924).

### Notes

The authors declare no competing financial interest.

#### REFERENCES

(1) Culliney, T. W. Crop Losses to Arthropods. In *Integrated Pest Management: Pesticide Problems*, Vol. 3; Pimentel, D., Peshin, R., Eds.; Springer: Dordrecht, The Netherlands, 2014; pp 201–225.

(2) Aktar, Md. W.; Sengupta, D.; Chowdhury, A. Impact of Pesticides Use in Agriculture: Their Benefits and Hazards. *Interdiscip. Toxicol.* **2009**, *2*, 1–12.

- (3) Nicolopoulou-Stamati, P.; Maipas, S.; Kotampasi, C.; Stamatis, P.; Hens, L. Chemical Pesticides and Human Health: The Urgent Need for a New Concept in Agriculture. *Front. Public Health* **2016**, *4*, 148.
- (4) Damalas, C. A.; Eleftherohorinos, I. G. Pesticide Exposure, Safety Issues, and Risk Assessment Indicators. *Int. J. Environ. Res. Public Health* **2011**, *8*, 1402–1419.
- (5) Vurro, M.; Miguel-Rojas, C.; Pérez-de-Luque, A. Safe Nanotechnologies for Increasing the Effectiveness of Environmentally Friendly Natural Agrochemicals. *Pest Manage. Sci.* **2019**, *75*, 2403–2412.
- (6) Nuruzzaman, Md.; Rahman, M. M.; Liu, Y.; Naidu, R. Nanoencapsulation, Nano-Guard for Pesticides: A New Window for Safe Application. *J. Agric. Food Chem.* **2016**, *64*, 1447–1483.
- (7) Chariou, P. L.; Ortega-Rivera, O. A.; Steinmetz, N. F. Nanocarriers for the Delivery of Medical, Veterinary, and Agricultural Active Ingredients. *ACS Nano* **2020**, *14*, 2678–2701.
- (8) Cao, J.; Guenther, R. H.; Sit, T. L.; Lommel, S. A.; Opperman, C. H.; Willoughby, J. A. Development of Abamectin Loaded Plant Virus Nanoparticles for Efficacious Plant Parasitic Nematode Control. *ACS Appl. Mater. Interfaces* **2015**, *7*, 9546–9553.
- (9) Chariou, P. L.; Dogan, A. B.; Welsh, A. G.; Saidel, G. M.; Baskaran, H.; Steinmetz, N. F. Soil Mobility of Synthetic and Virus-Based Model Nanopesticides. *Nat. Nanotechnol.* **2019**, *14*, 712–718.
- (10) Chariou, P. L.; Steinmetz, N. F. Delivery of Pesticides to Plant Parasitic Nematodes Using Tobacco Mild Green Mosaic Virus as a Nanocarrier. *ACS Nano* **2017**, *11*, 4719–4730.
- (11) Charudattan, R.; Hiebert, E. A Plant Virus as a Bioherbicide for Tropical Soda Apple, Solanum Viarum. *Outlooks Pest Manage.* **2007**, *18* (18), 167–171.
- (12) Charudattan, R.; Pettersen, M. S.; Hiebert, E. Use of Tobacco Mild Green Mosaic Virus (TMGMV) Mediated Lethal Hypersensitive Response (HR) as a Novel Method of Weed Control. US7494955, 2009.
- (13) Ross, A. F.; Stanley, W. M. The Partial Reactivation of Formalized Tobacco Mosaic Virus Protein. *J. Gen. Physiol.* **1938**, 22, 165–191.
- (14) Bawden, F. C.; Kleczkowski, A. The Behaviour of Some Plant Viruses after Exposure to Ultraviolet Radiation. *J. Gen. Microbiol.* **1953**, *8*, 145–156.
- (15) Cartwright, T. E.; Ritchie, A. E.; Lauffer, M. A. The Reaction of Tobacco Mosaic Virus with Formaldehyde: Kinetics of the Loss of Infectivity. *Virology* **1956**, *2*, 689–702.
- (16) Ginoza, W.; Siegel, A.; Wildman, S. G. Sensitivity to Ultra-Violet Light of Infectious Tobacco Mosaic Virus Nucleic Acid. *Nature* **1956**, *178*, 1117–1118.
- (17) McLaren, A. D.; Takahashi, W. N. Inactivation of Infectious Nucleic Acid from Tobacco Mosaic Virus by Ultraviolet Light. *Radiat. Res.* 1957, 6, 532–542.
- (18) Rushizky, G. W.; Knight, C. A.; McLaren, A. D. A Comparison of the Ultraviolet-Light Inactivation of Infectious Ribonucleic Acid Preparations from Tobacco Mosaic Virus with Those of the Native and Reconstituted Virus. *Virology* **1960**, *12*, 32–47.
- (19) Goddard, J.; Streeter, D.; Weber, C.; Gordon, M. P. Studies on the Inactivation of Tobacco Mosaic Virus by Ultraviolet Light. *Photochem. Photobiol.* **1966**, *5*, 213–222.
- (20) Streeter, D. G.; Gordon, M. P. Ultraviolet Photoinactivation Studies on Hybrid Viruses Obtained by the Cross-Reconstitution of the Protein and RNA Components of U(1) and U(2) Strains of TMV. *Photochem. Photobiol.* **1967**, *6*, 413–421.
- (21) Kleczkowski, A.; McLaren, A. D. Inactivation of Infectivity of RNA of Tobacco Mosaic Virus during Ultraviolet-Irradiation of the Whole Virus at Two Wavelengths. *I. Gen. Virol.* **1967**, *1* (4), 441–448.
- (22) Umekawa, M.; Oshima, N. Sensitivity of Tobacco Mosaic Virus to Ultraviolet Irradiation. *Jpn. J. Microbiol.* **1972**, *16*, 441–443.
- (23) Rae, C.; Koudelka, K. J.; Destito, G.; Estrada, M. N.; Gonzalez, M. J.; Manchester, M. Chemical Addressability of Ultraviolet-Inactivated Viral Nanoparticles (VNPs). *PLoS One* **2008**, *3*, e3315.
- (24) Niu, Z.; Bruckman, M.; Kotakadi, V. S.; He, J.; Emrick, T.; Russell, T. P.; Yang, L.; Wang, Q. Study and Characterization of

- Tobacco Mosaic Virus Head-to-Tail Assembly Assisted by Aniline Polymerization. *Chem. Commun.* **2006**, No. 28, 3019–3021.
- (25) Chariou, P. L.; Beiss, V.; Ma, Y.; Steinmetz, N. F. In Situ Vaccine Application of Inactivated CPMV Nanoparticles for Cancer Immunotherapy. *Mater. Adv.* **2021**, *2*, 1644–1656.
- (26) Furuya, Y.; Regner, M.; Lobigs, M.; Koskinen, A.; Mullbacher, A.; Alsharifi, M. Effect of Inactivation Method on the Cross-Protective Immunity Induced by Whole "killed" Influenza A Viruses and Commercial Vaccine Preparations. *J. Gen. Virol.* **2010**, *91*, 1450–1460.
- (27) Henderson, E. E.; Tudor, G.; Yang, J.-Y. Inactivation of the Human Immunodeficiency Virus Type I (HIV-1) by Ultraviolet and X Radiation. *Radiat. Res.* **1992**, *131*, 169–176.
- (28) Jean, J.; Morales-Rayas, R.; Anoman, M.-N.; Lamhoujeb, S. Inactivation of Hepatitis A Virus and Norovirus Surrogate in Suspension and on Food-Contact Surfaces Using Pulsed UV Light (Pulsed Light Inactivation of Food-Borne Viruses). *Food Microbiol.* **2011**, 28, 568–572.
- (29) Uittenbogaard, J. P.; Zomer, B.; Hoogerhout, P.; Metz, B. Reactions of Beta-Propiolactone with Nucleobase Analogues, Nucleosides, and Peptides: Implications for the Inactivation of Viruses. *J. Biol. Chem.* **2011**, 286, 36198–36214.
- (30) Wilton, T.; Dunn, G.; Eastwood, D.; Minor, P. D.; Martin, J. Effect of Formaldehyde Inactivation on Poliovirus. *J. Virol.* **2014**, 88, 11955.
- (31) Campbell, T. M.; Studdert, M. J.; Blackney, M. H. Immunogenicity of Equine Herpesvirus Type 1 (EHV1) and Equine Rhinovirus Type 1 (ERhV1) Following Inactivation by Betapropiolactone (BPL) and Ultraviolet (UV) Light. *Vet. Microbiol.* **1982**, *7*, 535–544.
- (32) Logrippo, G. A. Investigations of the Use of Beta-Propiolactone in Virus Inactivation. *Ann. N. Y. Acad. Sci.* **1960**, *83*, 578–594.
- (33) Race, E.; Stein, C. A.; Wigg, M. D.; Baksh, A.; Addawe, M.; Frezza, P.; Oxford, J. S. A Multistep Procedure for the Chemical Inactivation of Human Immunodeficiency Virus for Use as an Experimental Vaccine. *Vaccine* 1995, 13, 1567–1575.
- (34) Budowsky, E. I.; Friedman, E. A.; Zheleznova, N. V.; Noskov, F. S. Principles of Selective Inactivation of Viral Genome: Inactivation of the Infectivity of the Influenza Virus by the Action of  $\beta$ -Propiolactone. *Vaccine* **1991**, *9*, 398–402.
- (35) Frösner, G. G.; Stephan, W.; Dichtelmüller, H. Inactivation of Hepatitis A Virus Added to Pooled Human Plasma by Beta-Propiolactone Treatment and Ultraviolet Irradiation. *Eur. J. Clin. Microbiol.* **1983**, *2*, 355–357.
- (36) Fan, Y.-C.; Chiu, H.-C.; Chen, L.-K.; Chang, G.-J. J.; Chiou, S.-S. Formalin Inactivation of Japanese Encephalitis Virus Vaccine Alters the Antigenicity and Immunogenicity of a Neutralization Epitope in Envelope Protein Domain III. *PLoS Neglected Trop. Dis.* **2015**, *9*, e0004167.
- (37) Takada, A.; Matsushita, S.; Ninomiya, A.; Kawaoka, Y.; Kida, H. Intranasal Immunization with Formalin-Inactivated Virus Vaccine Induces a Broad Spectrum of Heterosubtypic Immunity against Influenza A Virus Infection in Mice. *Vaccine* **2003**, *21*, 3212–3218.
- (38) Kissling, R. E.; Reese, D. R. Anti-Rabies Vaccine of Tissue Culture Origin. *J. Immunol.* **1963**, *91*, 362.